Journal of Applied Mechanics and Technical Physics, Vol. 40, No. 6, 1999

MODEL FOR PLASTICITY EFFECTS IN METALS UNDER NONPROPORTIONAL CYCLIC LOADING

I. É. Keller and P. V. Trusov

UDC 539.374

A possible physical mechanism for additional hardening is proposed on the basis of an analysis of experiments on nonproportional cyclic loading of metals. A model for an elastoplastic polycrystal with a hardening law taking into account the interaction of slip systems is developed. The effect of additional hardening for elliptic strain paths and the shapes of stress paths and hysteresis loops typical of elliptic strain paths are described qualitatively. A violation of the assumption of the local determinacy and orientations of stress paths is considered for the square strain paths taking place in tests of chromium–nickel austenite stainless steels.

Introduction. In real processes of plastic deformation of metallic polycrystals, any small material particle is subjected to complex loading even when components of the boundary forces and displacements change proportionally. This is due to the complex geometry of the surface on which the boundary conditions are specified and (from a physical point of view) to the presence of internal boundaries separating crystallites in the body. The local plastic properties of some widely used metals under *nonproportional cyclic* loading are characterized by a number of effects not found in nonproportional monotonic and proportional cyclic types of loadings [1–4]. The difficulties in deriving constitutive elastoplastic relations for complex cyclic loading, which are noted by all specialists (see, for example, [5–7]), motivate the necessity of choosing a physically justified structure of these relations and the study of the causes and physical mechanism of the phenomenon. The paper presents a mathematical model that describes the effect of additional hardening and a number of other plasticity effects in nonproportional cyclic loading of macrohomogeneous specimens.

1. Effect of Additional Hardening in Nonproportional Cyclic Loading. Results of systematic experimental studies of the local plastic properties of metals with variation in the shape of cyclic strain paths are given in [1–4]. The object of research was a thin-walled tubular specimen subjected to compression–tension and alternating torsion (P–M experiments [7]). Symmetric periodic actions, shown by phase paths in the two-dimensional strain subspace $e_1 = \varepsilon$ and $e_2 = \gamma/\sqrt{3}$ (ε is the axial strain and γ is the torsional strain), were delivered to the longitudinal and torsional operating mechanisms. Tanaka et al. [1] studied elliptic paths in the subspace of total strains, and Ishikawa and Sasaki [2] studied various closed paths in the subspace of plastic strains. In studies of the relationship between the plastic properties and the strain path shape, the maximum intensities of cyclic strains e_+ were fixed in corresponding series of experiments. The tests were performed at room temperature, and the strain rate was varied in the range from 10^{-4} to 10^{-3} sec^{-1}. In the initial state, the specimen material was isotropic.

The experiments showed some new properties of the tested materials in a cyclically stabilized state. In particular, for a number of metals, additional hardening was found to depend strongly on the strain path shape. For chromium–nickel austenite stainless steel AISI 304 subjected to deformation in the elliptic paths [1] $e_1 = e_+\sqrt{2}(1+\delta^2)^{1/2}\cos(\theta+\varphi)$, $e_2 = e_+\sqrt{2}(1+\delta^2)^{1/2}\cos(\theta-\varphi)$, $\delta = \tan\varphi = e_-/e_+$, and $\theta = \omega t$ with

Perm' State Technical University, Perm' 614600. Translated from Prikladnaya Mekhanika i Tekhnicheskaya Fizika, Vol. 40, No. 6, pp. 144–151, November–December, 1999. Original article submitted July 22, 1998

TABLE 1

Material	σ_Y, MPa	σ_P, MPa	σ_{NP}, MPa
Al	36	55	55
Ni	245	370	420
Cu	100	190	220
SUS 304	250	420	620

major semiaxis $e_+ = 0.005$ and ratios of the axes $\delta = 0$, 0.25, 0.5, 0.75, and 1, the corresponding maximum stress intensity in the cycle σ_∞ were equal to 296, 320, 340, 425, and 460 MPa, respectively. The experiments of [2] with steel of the same class AISI 316 deformed in paths of fixed radius $e_+^p = 0.002$ and various shapes in the plastic strain subspace also showed that the values of σ_∞ depended on the shape of the cyclic paths: 300 MPa for proportional paths, 405 for cross-shaped paths, 435 for star-shaped paths, 470 for square paths, and 485 MPa for circular paths. Maximum cyclic hardening in both cases was reached for circular strain paths. McDowell [6] refers to experiments in which the value of σ_∞ for a circular path was 75–80% higher than that for a proportional path. Itoh et al. [3] studied the tendency toward additional cyclic hardening for a number of metals subjected to proportional and nonproportional (in a cross-shaped path) cyclic deformation in the total strain subspace ($e_+ = 0.004$–0.008). Results of the investigation are given in Table 1 (σ_Y is the initial yield strength and σ_P and σ_{NP} are the corresponding values of σ_∞ for deformations in proportional and nonproportional cross-shaped paths).

Other important characteristics of the loading type considered are a violation [2] of the Lenskii assumption of local determinacy [7], the peculiar type of elastoplastic hysteresis loops (see, for example, [2]), and incomplete cyclic softening in programs including stages of nonproportional and proportional cyclic deformation [1].

2. Probable Physical Mechanism of the Effect. Analyzing 13 published experimental studies for different metals and alloys, we [8] established that all metals and solid solutions that were sensitive to the path shape of cyclic strains had a face-centered cubic (FCC) lattice, and the main mechanism of inelastic deformation was a crystallographic slip that allowed only a simple shear by 12 slip systems. A comparison of the tendency of metals toward additional hardening at various homologous temperatures (ratio of the experiment temperature to the melting point in Kelvin) suggested that this effect is athermal.

Itoh [3] performed an experimental investigation of the correlation between the measure of additional hardening $\eta \equiv (\sigma_{NP} - \sigma_Y)/(\sigma_P - \sigma_Y)$ and the energy of a crystal-lattice defect in a metal or an alloy. The data of [3] confirmed our assumption [9] that the measure of additional hardening correlates with the dimensionless complex $\Gamma \equiv \gamma_{SF}/(Gb)$, which is the ratio of the energy of the lattice defect γ_{SF} to the averaged shear modulus G and Burgers vector magnitude b. With decrease in this parameter, the value of the measure of additional hardening increases: $\eta \sim 1/\sqrt{\Gamma}$ (the experimental points and regression curves were plotted from the data of [3]). At the same time, the parameter $\mu \equiv \bar{d}_{NP}/\bar{d}_P$ of the sensitivity of a dislocation structure to the path shape of cyclic loading shows the dependence $\mu \sim \sqrt{\Gamma}$, where $\bar{d}_P$ and $\bar{d}_{NP}$ are the averaged diameters of cells of the dislocation structure in proportional and nonproportional cyclic deformation. Decreasing Γ decreases the averaged dimensions of the fragment of the dislocation structure after nonproportional cyclic deformation in comparison to those after proportional cyclic deformation.

In the case of a split dislocation, the dimensionless energy of the lattice defect is inversely proportional to the width of the lattice defect normalized to the atomic size. The rather small value of the parameter corresponds to widely split dislocations, and this hinders all processes that require compression of the dislocations, including the processes of destruction of dislocation barriers. For this reason, in metals with a small value of Γ, hardening occurs due to formation of Lomer–Cottrell dislocation barriers [10] in the interaction of dislocations belonging to particular pairs of slip systems. In a nonproportional deformation cycle, particularly of a form such that the strain tensors and the strain rate tensors are nonproportional at each

time (circular and square strain paths), the interaction of particular pairs of slip systems leads to formation of the above-mentioned strong dislocation barriers. Thus, a probable mechanism for the effect of additional hardening is the formation of strong Lomer–Cottrell dislocation barriers.

3. Model. To take into account the proposed hardening mechanism at the lattice level in the constitutive equations, we develop the following model. A polycrystalline specimen is imagined as a set of elastoplastic single crystals (grains) with certain orientation. It is assumed that the elastic properties of the grains are identical and have cubic symmetry, and the plastic properties are anisotropic with an anisotropic hardening law ignoring translation. To join the grains in a unit, we assumed that the rate tensor of total strains of the specimen is equal to the same tensors of each grain. The stress tensor in the specimen is determined as the mean over the grains making up the aggregate with a certain distribution density function $f(\tau_*)$, where τ_* is the initial yield stress of the slip system. All grains are arranged in groups, in each of which the initial plastic properties of the grains are identical and their orientations are distributed under a uniform law for the initial isotropy of the material.

For the single crystals making up the aggregate, constitutive elastoplastic relations are formulated that take into account the slip mechanism by the slip systems of a FCC crystal and the possibility of different isotropic hardening of these systems [the critical shear stresses τ_*^k $(k = 1, \ldots, 12)$ may not be equal]:

$$\dot{E} = \dot{E}^* + \dot{\tilde{E}}; \tag{1}$$

$$\dot{E}^* = pq(q-1)A : \dot{S}; \tag{2}$$

$$\dot{\tilde{E}} = j\dot{\lambda}qA : S, \qquad j = \begin{cases} 1 & \text{for} \quad F(S) = \nu, \quad dF(S) = 0, \\ 0 & \text{for} \quad F(S) < \nu \quad \text{or} \quad F(S) = \nu, \quad dF(S) < 0. \end{cases} \tag{3}$$

Here

$$F(S) \equiv \sum_{k=1}^{12} \left| \frac{S : M_k}{\tau_*^k} \right|^q, \qquad A \equiv \frac{1}{q(q-1)} \frac{\partial^2 F(S)}{\partial S^2} = \sum_{k=1}^{12} \frac{M_k}{\tau_*^k} \left| \frac{S : M_k}{\tau_*^k} \right|^{q-2} \frac{M_k}{\tau_*^k}, \tag{4}$$

Here S is the stress deviator, E and E^* and $\tilde{E}$ are the deviator tensors of small strains and its elastic and plastic parts, respectively, and M_k is a symmetric dyad that specifies the kth slip system of a FCC-crystal $(k = 1, \ldots, 12)$ and is also a deviator:

$$\dot{\tilde{E}} = \dot{\gamma}^k M_k, \tag{5}$$

and $q \geqslant 2$ is a parameter that determines the shape of the yield surface together with the exponent of the hyperelastic potential. Defining the constant ν, which depends on q, by $\nu = F(\tau_* M_k)$, we have 24 general points of the yield surface $F(S) = \nu$ and the Bishop–Hill polyhedron that correspond to the cases of a single slip. The yield function $F(S)$ allows for the contribution of all normalized stresses $S : M_k$ $(k = 1, \ldots, 12)$, and the corresponding criterion predicts the beginning of yield at the moment the energy of reversible deformations (2) reaches a limiting value. The constant q determines the initial shape of the yield surface of the single crystal, and p determines the slope of the curve of uniaxial tension of the single crystal along the axis of the cube at the moment preceding the beginning of yield. Equations (1)–(4) are derived and analyzed in [11].

The rate of plastic shear by the kth slip system $\dot{\gamma}^k$ is obtained from the gradient law in terms of normalized stresses and shears by the slip systems:

$$\dot{\gamma}^k \equiv \dot{\lambda} \frac{\partial F(S : M_k)}{\partial (S : M_k)} = \dot{\lambda} q \frac{S : M_k}{\tau_*^k} \left| \frac{S : M_k}{\tau_*^k} \right|^{q-2} \frac{1}{\tau_*^k} \tag{6}$$

[which, combined with (5), leads to (3)]. In (6), summation over k is not performed.

The hardening law for the kth slip system is adopted in the form

$$\tau_*^k = \tau_* + \alpha^k(\tau_*^k), \tag{7}$$

where α^k is the cyclic-hardening parameter for the kth slip system, which depends on τ_*^k. The first term on the right side of (7) is due to internal friction, and the second corresponds to deformation cyclic hardening and can be due to the resistance of statistically isotropic dislocation structures. Depending on the history of cyclic deformation, a dislocation structure is adjusted to the action, and this results in hardening or softening ($\tau_*^k \geqslant \tau_*$, however). The expression for the measure α^k is written as

$$\alpha^k = \int_0^t g^k(t) \exp\left(-æ(\chi^k(t) - s(t))\right) ds\,(t), \tag{8}$$

and it takes into account the "forgetting" of local hardening acts (such as transverse hardening upon a sharp change in orientation of the strain path), which took place in the experiments of [1]. In (8), t is a deformation parameter, $æ$ is a relaxation factor, $0 \leqslant s \leqslant \chi^k$, where χ^k is the accumulated plastic shear by the kth slip system

$$\chi^k(t) = \int_0^t |\dot{\gamma}^k(t)|\, dt,$$

and $g^k(t)$ is a hardening function for the kth slip system, written as

$$g^k(t) = H\Big[(1 - \exp(-\xi\chi^k)) + B\sum_{j(k)} h(\dot{\gamma}^k\dot{\gamma}^j)|\gamma^k|\,|\gamma^j|\Big]. \tag{9}$$

The first term in (9) allows for the self-hardening of the slip system in proportional cyclic deformation (when the interaction of the systems is insignificant). The constants H and ξ determine the hardening and the rate of hardening, respectively in this process, and the constant B is the hardening due to formation of dislocation barriers. The formula for the measure (8) and the function (9) contain plastic shears and their rates. Plastic deformations are observed during the part of the cycle where the point representing the stress state is on the yield surface. Therefore, the measure $\alpha^k(\tau_*^k)$ in (7) depends on the yield stress. A hardening law similar to (7) is adopted in the model of [12] for a structural element within the framework of a version of the statistical Kadashevich–Novozhilov model, which differs, in addition, by the choice of the hardening parameter. In [12], the hardening parameter was the work of plastic distortion of the structural element over the last cycle, which depends, as well as the measure $\alpha^k(\tau_*^k)$, on the current yield stress.

A study of the geometry of the Lomer–Cottrell reaction [10] shows that the slip systems of a FCC single crystal are arranged in four nonoverlapping groups so that the barrier forms only in the interaction of a pair of slip systems of the same group. The corresponding reaction takes place for a particular combination of the signs of the Burgers vectors and directions of dislocation motion (in other words, for appropriate configurations of simple shears) of the interacting slip systems. The symmetric dyads of slip systems can be oriented so that three such dyads of any group form a closed loop in the space of symmetric deviators. Therefore, the criterion for formation of the barriers is written in the above function (9) using the Heaviside function $h(x)$; in (9), $j(k)$ is the index of the group of Lomer–Cottrell slip systems that includes the kth system.

To describe P–M experiments, we write all relations of the model in terms of the strain subspaces $e_1 = \varepsilon$ and $e_2 = \gamma/\sqrt{3}$ (ε is the axial strain and γ is the torsional strain) and the stress subspace $s_1 = \sigma$ and $s_2 = \tau/\sqrt{3}$ (σ is the axial strain and τ is the torsional stress) of the corresponding Il'yushin's vector spaces E_5 and Σ_5 [7]. Below, we consider a simplified (hypothetical) model of a polycrystal in which each single crystal has slip systems represented by three unit vectors forming a closed loop in the two-dimensional subspace considered. All the results given below were obtained for $q = 2$, i.e., the initial shape of the yield curve of the single crystals in the subspace s_1, s_2 was circular. The aggregate contained n groups of grains in each of which the elements have different orientations but the same initial radius of yield circles. Using the method of [13], from the uniaxial tensile curves for stainless steels AISI 304 and AISI 316 in intensities taken from [2] and [4], respectively, we determined the initial yield strengths and weights of the grains and the

TABLE 2

AISI 304		AISI 316	
τ_*	f	τ_*	f
165.0	0.350	90.0	0.2800
190.4	0.306	155.4	0.2410
249.0	0.135	245.4	0.1370
304.6	0.083	360.0	0.1040
412.5	0.041	482.7	0.0652
498.2	0.028	605.4	0.0431
609.1	0.021	777.2	0.0330
747.2	0.013	998.1	0.0339
996.3	0.009	1210.8	0.0293
1245.0	0.008	1472.6	0.0318
1495.0	0.006		

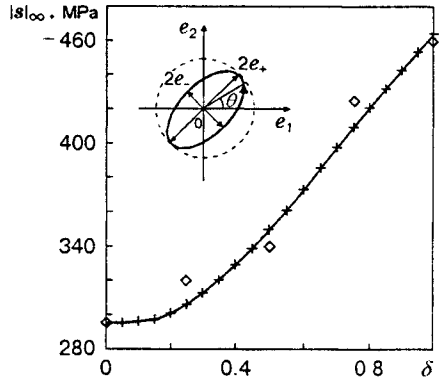

Fig. 1

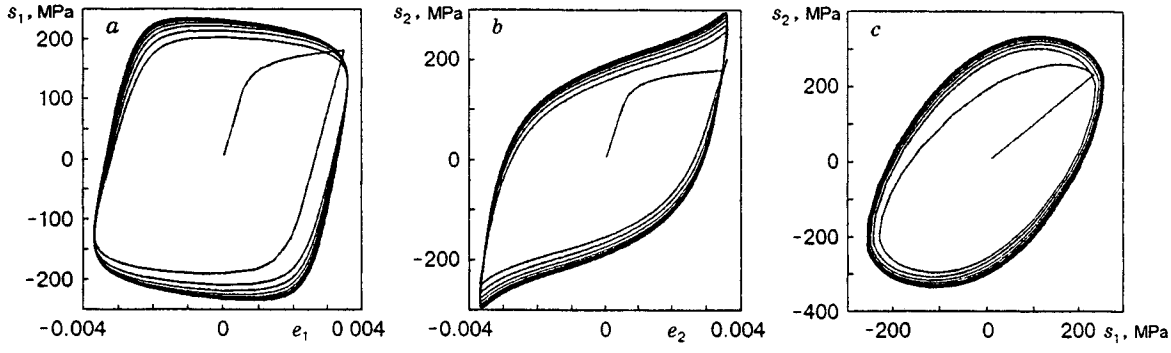

Fig. 2

elastic moduli of the materials. In this version of the model, the initial yield strengths of the grains coincide with τ_*, and (3) takes the form $\dot{s} = 3G\dot{e}$. Table 2 gives the values of τ_* (in megapascals) and f for AISI 304 ($n = 11$ and $3G = 245.4$ GPa) and AISI 316 ($n = 10$ and $3G = 199.2$ GPa). The remaining parameters for both materials (similar in plastic properties) $æ = 50$, $\xi = 2 \cdot 10^4$, $H = 2 \cdot 10^9$ Pa, and $B = 1.4 \cdot 10^6$ were selected so as to describe the effect of additional hardening on elliptic paths of cyclic deformation.

4. Results and Discussion Figure 1 gives the cyclic hardening $|s|_\infty$ of steel AISI 304 deformed in elliptic paths that are equally sloped to the e_1 and e_2 axes, with the unchanged major semiaxis $e_+ = 0.005$ versus the ratio of the semiaxes of the ellipse δ calculated using the model. The diamonds show the experimental data of [1] and the crosses show the calculation results. It follows from Fig. 1 that the hardening function (9) and the "forgetting" measure (8) allow one to describe the inflection point on the experimental curve. The calculation of this curve is stable with respect to small changes in the parameters of the material q, $æ$, ξ, H, and B.

Figure 2 shows calculated curves of elastoplastic hysteresis (Fig. 2a and b) and the stress path (Fig. 2c) for the same elliptic path of cyclic deformation with $\delta = 0.25$ of steel AISI 304. The curves in Fig. 2a and b, calculated using the proposed model, have the following features: one of the hysteresis loops (Fig. 2a) has a rounded shape and descending segments and the other (Fig. 2b) has a sharp shape and concave segments. The loops obtained experimentally under similar conditions [2] have the same typical shapes. Even in the first studies of nonproportional cyclic plasticity, it was noted that the hysteresis loops for this type of loading differed qualitatively in shape from the loops in proportional cyclic deformation. It is known that the shape and dimensions of the hysteresis loops characterize the amount of energy absorbed by the material during cyclic deformation, and part of the energy is accumulated as the internal (elastic) energy of the

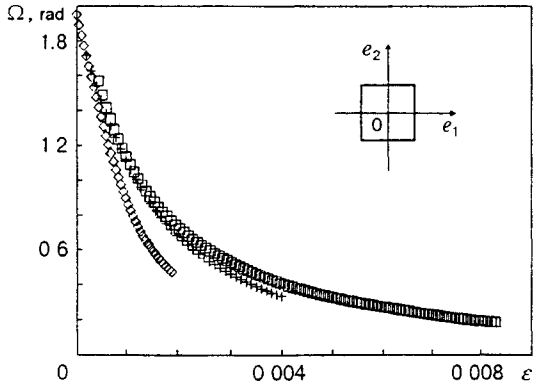

Fig. 3

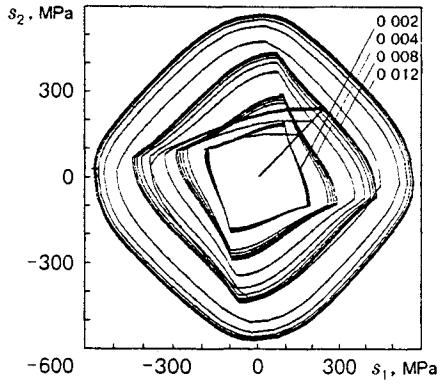

Fig. 4

dislocation structure. A theoretical description of the shape and dimensions of hysteresis loops as functions of the properties of the material and the cyclic deformation path is important in studies of low-cycle fatigue. Figure 2c shows the stress path, which is in good qualitative agreement with the experimental curve of [2].

Figure 3 gives calculated curves of the angle of approach Ω of the stress vectors and the strain rate vectors after the inflection point versus the length of the arc of the path of total strains ε for the cyclic deformation of steel AISI 316 in square paths. Diamonds, crosses, and squares show the results obtained for squares 0.002, 0.004, and 0.008 on a side, respectively. The difference between the curves corresponds to a violation of the assumption of local determinacy [7] since the length of the side of the square is not among the local parameters of the process. This distinguishing feature of cyclic nonproportional plasticity was noted for the first time in [4], where similar experimental dependences are given.

Figure 4 gives stress paths that correspond to the cyclic deformation of steel AISI 316 in square paths (see Fig. 3) with squares 0.002, 0.004, 0.008, and 0.012 on a side. The experimental data of [4] show that the symmetry axes of the stress paths are rotated about the symmetry axes of the square strain path. The angle of rotation of the symmetry axes increases with increase in the length of the side of the square strain path. The calculated paths (Fig. 4) have the same peculiarity. This indicates that the model provides a qualitative description of the vectorial and scalar properties of the material [7] that are jointly responsible for the effect.

Although the model describes a number of peculiarities of nonproportional cyclic plasticity, the question of whether it is adequate for describing the dependence of cyclic hardening on the strain path shape (paths having the shape of crosses, stars, butterflies, etc. [1]) is still open. Calculation results for such paths are not given here because in the experiments of [1] plastic deformations were studied, whereas the proposed algorithm of implementation of the model is intended for total deformations, and it is not quite correct to compare these results.

The problem of the incomplete "forgetting" of the cyclic deformation history (including incomplete cyclic softening), which is also typical of nonproportional cyclic deformation [1], remains to be solved.

In conclusion, we emphasize the importance of a comparison between various approaches to deriving constitutive equations for complex cyclic loading, including the approach described in the present paper. Almost all existing models of the phenomenon considered are based on modifications of the two-surface theories of plastic yield in terms of the stress space and/or strain space (see [6, 14]) or the endochronous theory of plasticity [15]. It may be useful to reject the macrodeterminacy hypothesis and to describe the macroproperties of materials in correlation with the structures developing in it.

This work was supported by the Russian Foundation for Fundamental Research (Grant No. 98-01-00125).

REFERENCES

1. E. Tanaka, S. Murakami, and M. Ooka, "Effect of strain paths shape on nonproportional cyclic plasticity," *J. Mech. Phys. Solids*, **33**, No. 6, 559–575 (1985).
2. H. Ishikawa and K. Sasaki, "Application of the hybrid constitutive model for cyclic plasticity to sinusoidal loading," *Trans. ASME, J. Eng. Mater. Technol.*, **114**, No. 2, 172–179 (1992).
3. T. Itoh, M. Sakane, M. Ohnami, and K. Ameyama, "Effect of stacking fault energy on cyclic constitutive relation under nonproportional loading," *J. Soc. Mater. Sci.*, **41**, No. 468, 1361–1367 (1992).
4. Y. Ohasi, E. Tanaka, and M. Ooka, "Plastic deformation behavior of type 316 stainless steel subject to out-of-synphase strain cycles," *J. Eng. Mater. Technol.*, No. 4, 286–292 (1985).
5. Yu. I. Kadashevich and S. P. Pomytkin, "The nonproportionality effect in complex cyclic loading," in: *Applied Problems of Strength and Plasticity: Numerical Simulation of Physicomechanical Processes* (Collected scientific papers) [in Russian], Izd. Mosk Univ., Moscow (1995), pp. 171–175.
6. D. L. McDowell, "An evaluation of recent developments in hardening and flow rules for rate-independent, nonproportional cyclic plasticity," *Trans. ASME, Ser. E, J. Appl. Mech.*, **54**, No. 2, 323–334 (1987).
7. R. A. Vasin, "Constitutive relations of the theory of plasticity," *Itogi Nauki Tekh., Ser. Mekh. Deform. Tverd. Tela*, **21**, 3–75 (1990).
8. I. É. Keller, "Nonproportional cyclic plasticity: Physical analysis and simulation," Candidate's Dissertation in Phys.-Math. Sci., Perm' (1997).
9. P. V. Trusov, I. E. Keller, and V. D. Oniskiv, "On constitutive relations of plasticity under nonproportional cyclic loading," in: *Influence of Microstructure on the Constitutive Equations in Solids*: Proc. EUROMECH Colloq. 303 (Moscow–Perm', May 11–19, 1993) Perm' (1993), p. 28.
10. J. P. Hirth, "On dislocation interactions in the FCC lattice," *J. Appl. Phys.*, **32**, No. 4, 700–706 (1961).
11. I. É. Keller and P. V. Trusov, "Generalization of the Bishop–Hill theory of plastic distortion of a single crystal," *Izv. Ross. Akad. Nauk, Mekh. Tverd. Tela*, No. 6, 93–103 (1997).
12. I. É. Keller and P. V. Trusov, "Simple elastoplastic model for nonproportional cyclic loading," *Probl. Prochn.*, No. 1, 15–24 (1998).
13. I. E. Keller, V. G. Kuznetsova, and R. S. Novokshanov, "Comparison of two elastoplastic models extending the Masing model to the case of complex loading," in: *Mathematical Simulation of Systems and Processes* (Collected scientific papers) [in Russian], No. 4, Izd. Perm' Tekh. Univ., Perm' (1996), pp. 29–39.
14. E. Tanaka,"A nonproportionality parameter and a cyclic viscoplastic constitutive model taking into account amplitude dependences and memory effects of isotropic hardening," *Eur. J. Mech. A. Solids*, **13**, 155–165 (1994).
15. N. K. Kucher and M. V. Borodii, "Version of the endochronous theory of plasticity for describing complex histories of cyclic loadings," *Probl. Prochn.*, No. 5, 3–12 (1993).